Research Article **Open Access**

Monika W. Staszek* and Mateusz J. Moskalik

Contemporary sedimentation in the forefield of Hornbreen, Hornsund

DOI 10.1515/geo-2015-0042

Received August 14, 2014; accepted December 11, 2014

Abstract: The paper presents a model of contemporary sedimentation in the forefield of Hornbreen, tidewater glacier in Brepollen. The model is based on the results of grain-size analyses of bottom sediments and the information about dominant sedimentary processes in glaciated fjords. It is concluded that apart from the tidewater glacier which is the main source of sediment in this area, the material is transported also from the shores. Subsequently, the material is redeposited by iceberg-caused reworking, slides and gravity flows. Strong decreasing trend of particles' diameters with increasing distance from the ice cliff is observed.

Keywords: Brepollen, Hornbreen; glaciomarine sediments; grain-size analysis; sedimentary processes

1 Introduction

Due to the climate warming since the end of the Little Ice Age, the retreat of most glaciers has been observed in Svalbard during 20th century [1–6]. This process is visible especially on the example of tidewater glaciers which terminating in water are more affected by temperature changes than other glaciers. Tidewater glaciers are affected by climate warming through changes in the surface mass balance components and the dynamic response of a glacier, as well as in case of glaciers of other types, but also through the influence of warmer water on the ice cliff [1]. The mean recession rate of tidewater glaciers in Hornsund during the last few decades varied from 20 m a^{-1} to 50 m a^{-1} [3], however, other tidewater glaciers of Svalbard are retreating with the speed up to 260 m a-1 [1, 6]. The average recession rate calculated for all tidewater glaciers of Svalbard equals about 30 m a^{-1} [1]. Retreating tidewater glaciers release huge amounts of meltwater and icebergs loaded with sediment which is accumulated in their forefields. The result of these processes is a significant increase of sediment accumulation rate (SAR). It has been estimated that in Hornsund SAR is generally in the range of 0.36-0.59 cm a^{-1} [7]. In Brepollen it reaches probably the highest value due to the big amount of tidewater glaciers concentrated in a small area.

Glaciomarine environments are complicated systems of deposition, because of superimposition of glacial and marine processes [8]. Therefore, apart from direct deposition from the glacier front, deposition from meltwater flows, settling from suspension and 'rain-out' from icebergs which are connected with glaciers' recession, other sedimentary processes such as resedimentation by gravity flows, subaerial rock falls and mass flows, current reworking or shoreline and biological sedimentation should be taken into account [9, 10]. All mentioned processes influence deposition of sediment in the forefields of tidewater glaciers and condition its distribution.

The aim of this study is to describe sedimentary processes controlling deposition in the forefield of Hornbreen on the basis of the modern sediment distribution. In this purpose, grain-size analyses of surface sediments and short cores has been undertaken to provide data reflecting horizontal and vertical sediment variations.

Previously, bottom sediments in Brepollen area have been described in 1986 [11], 1987 [12] and 1991 [13]. Subsequently, sediments were investigated in 2007 during Norwegian marine-geological cruise, when swath-bathymetry survey, high-resolution seismic profiles and sediment sampling were undertaken [14]. However, no data obtained during this research and concerning Brepollen area has been published.

***Corresponding Author: Monika W. Staszek:** Institute of Geophysics, Polish Academy of Sciences, Department of Seismology, Księcia Janusza 64, 01-452 Warszawa, Poland, E-mail: mstaszek@igf.edu.pl

Mateusz J. Moskalik: Institute of Geophysics, Polish Academy of Sciences, Department of Polar and Marine Research, Centre for Polar Studies KNOW (Leading National Research Centre) Księcia Janusza 64, 01-452 Warszawa, Poland

2 Study area

Hornsund is the southernmost major fjord developed in the west coast of Spitsbergen and orientated along W-E direction. It is about 30 km long and 5-12 km wide with five secondary bays developed within its coastline, all bounded on tidewater glaciers. Hornbreen is one of the six tidewater glaciers terminating in Brepollen – the easternmost and innermost bay of Hornsund fjord (Figure 1A).

Brepollen is about 13 km long and its width varies from 1.7 km to 15 km. The mouth of the bay is formed by two capes: Treskelodden from the N and Meranpynten from the S (Figure 1A). There are six tidewater glaciers flowing into Brepollen: Hyrnebreen (NW), Storbreen (N), Hornbreen (NE), Svalisbreen (SE), Mendelejevbreen (S) and Chomjakovbreen (S). The area of Brepollen is directly influenced by fluctuations of glaciers' fronts positions. The bay has been developing quickly from the beginning of 20^{th} century, when it was relatively small and ended with a cliff of one tidewater glacier [2, 4, 15]. Bathymetry of Brepollen is also a clear reflection of glaciers' activity. According to previous works [16–18], eight various subbasins within the bay can be distinguished: 6 subaqueous valleys of present tidewater glaciers, central Brepollen subbasin and Treskelbukta subbasin (Figure 1B). The maximum depth of over 100 m has been observed in the central basin, while depth measured in the Hornbreen's subaqueous valley reaches over 90 m (Figure 1B). Hydrological conditions change seasonally: during spring and summer seasons thermal and saline water stratification occurs, whereas in winter the water masses mix in a large volume [11].

Hornbreen is a polythermal surge-type tidewater glacier located in the easternmost part of Brepollen. Together with Hambergbreen, Hornbreen builds a solid barrier between Hornsund and the Barents Sea [4]. Hornbreen's ice cliff is restricted by two big peninsulas situated in front of Mezenryggen (N) and Ostrogradskifjella (S) massifs (Figure 1A) and covered with moraine deposits. On the basis of field observations, four zones of the ice cliff can be distinguished (from NW): (A) strongly crevassed zone, (B) main meltwater outflow zone, (C) high cliff zone and (D) bay-shaped zone (Figures 1A, 2). Numerous tidewater caves which indicate probable locations of englacial tunnels' outlets, are visible in the NW part of the cliff (Figure 2). Furthermore, ground penetrating radar survey has revealed the existence of big subglacial tunnels inside the glacier [19]. Present thickness of Hornbreen varies between 100 and 200 m [4] and its retreat velocity, estimated to be 70±30 m a^{-1}, is classified as slow [1]. The glacier's catchment area is built mainly of Lower Cretaceous coarse-grained sandstones and shales of Helvetjafjellet and Carolinefjellet Formations [20]. Debris cover and various types of moraines are intensively forming on the active glacier ice as a result of landslides and solifluction [21].

Hornbreen's subaqueous glacial valley has an asymmetric relief. The southern part of the valley is shallower, so the main valley axis is located in its northern part, where depth exceeds 90 m (Figure 1B). As a result, the valley's bottom builds 30–40% of its entire width [17].

3 Materials and methods

Sediment sampling took place in August 2008 and was performed at 38 stations located in the forefield of Hornbreen at distances of about 0.5–6 km from its cliff (Figure 1A, Table 1). Sediment cores were collected using gravitational bottom sediment sampler from the rubber-boat. The cores were cut into 1 cm thick slices, packed and stored firstly in a freezer and then in a fridge in temperature of about 2°C. Slices were signed according to X/y–z scheme, where X is the core number and y–z sediment depth interval.

The distances between Hornbreen's cliff position and sampling stations were estimated as the average value of the distances in 2007 and 2009 (Table 1). The reason for such an approximation is the lack of data concerning the cliff position in 2008 (Figure 1A).

Additionally, one CTD (conductivity, temperature, depth) profile (Figure 3A) and one current profile (Figure 3B) were measured in the near proximity of Hornbreen's ice cliff in July 2008 (Figure 1A point C1). The water column hydrological properties were measured using Mini CTD Sensordata SD202 at intervals of 2 seconds. For the purpose of current measurements, Sensordata current-meter Mini SD 6000 was used.

From the cores located along the main longitudinal and transverse profiles (Figure 1A), hereinafter referred to as 'axial cores', each slice was analysed individually to investigate the vertical sediment grain-size diversity. From other cores 'surface samples', consisting of three surface slices, were prepared and analysed in order to present areal sediment diversity. The mass of samples, dried in 105°C, varied in the range of 7.240–24.895 g for single slices and 27.590–46.604 g for 'surface samples'. Cores 11, 12, 15 and 38 were rejected from the analysis because of sampling errors.

Samples from 'axial cores' were wet-sieved using 0.5 mm, 1 mm and 2 mm Fritsch sieves. Analysis of grains

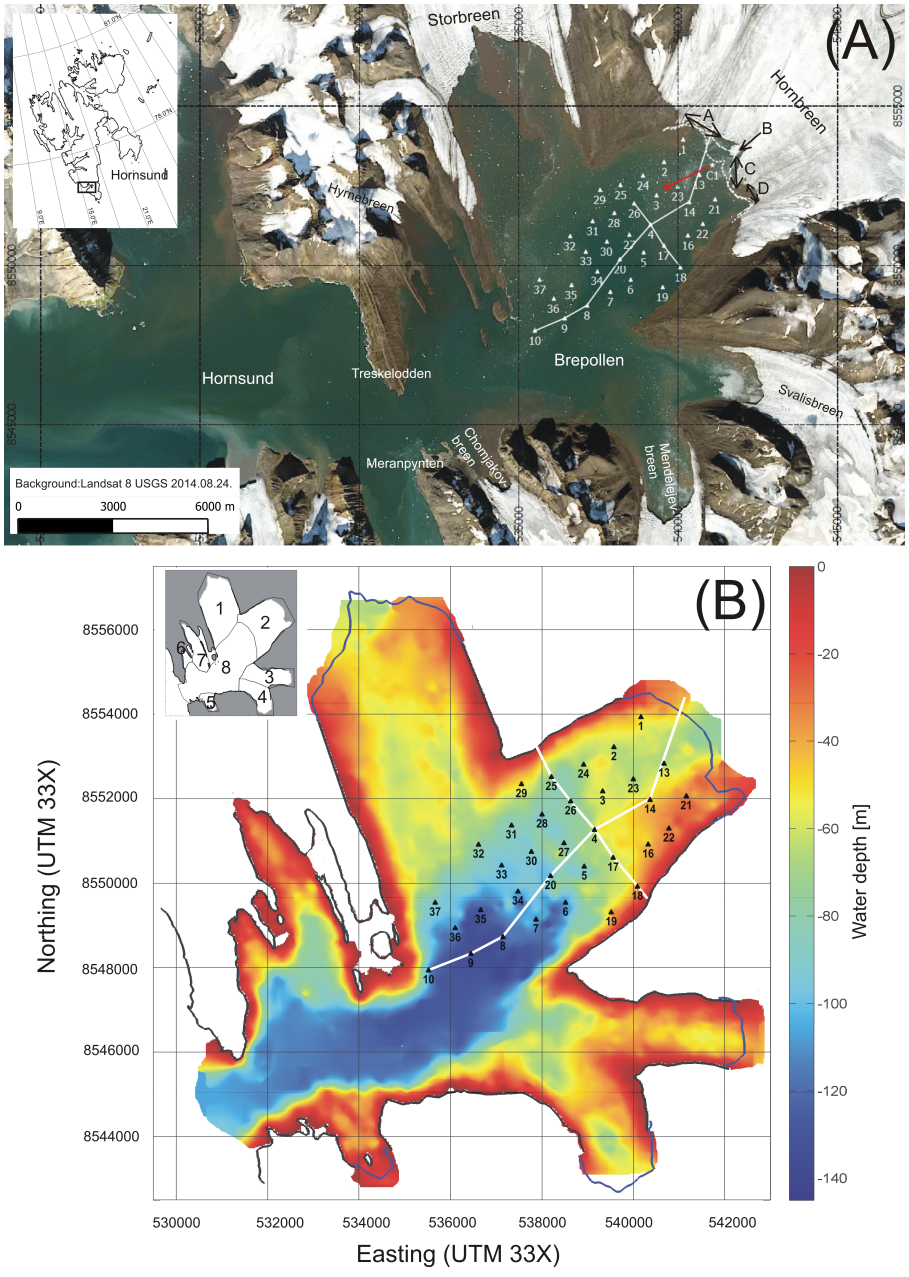

Figure 1: Study area: Brepollen, Hornsund, Svalbard. (A) Cores localization (white triangles), point of CTD profile and current measurements C1 (white star). White solid lines indicate longitudinal and transverse profiles, which include 'axial cores'. White dashed lines show positions of Hornbreen's ice cliff in 2007 (short dashed line) and 2009 (long dashed line). Black letters and arrows indicate zones distinguished within the ice cliff: A – strongly crevassed zone, B – main meltwater outflow zone, C – high cliff zone and D – permanent bay-shaped zone. Red arrow shows the direction of current measured at point C1. (B) Bathymetric map of Brepollen with visible coring stations (black triangles) and longitudinal and transverse profiles (white solid lines). Blue lines show positions of ice cliffs in 2010. Designated geographical units: 1 – Storbreen valley, 2 – Hornbreen valley, 3 – Svalisbreen valley, 4 – Mendelejevbreen valley, 5 – Chomjakovbreen valley, 6 – Treskelbukta, 7 – Hyrnebreen valley, 8 – Central Brepollen. Background satellite data collected by Landsat 8 on August 24, 2013, courtesy of the U.S. Geological Survey, Department of the Interior.

Table 1: Acquisition parameters of sediment cores collected from the forefield of Hornbreen. * indicates 'axial cores'. From the others 'surface samples' has been prepared.

Core number	Depth [m]	Length [cm]	Distance from the ice cliff in 2008 (estimated) [m]
1	55	11	426
2	unknown	7	1008
3	57	7	2061
4*	65	16	2652
5	77	14	3166
6	106	12	4050
7	117	21	4834
8*	128	23	5654
9*	136	9	6481
10	109	18	7461
13*	67	8	786
14*	47	14	1321
16	46	16	1744
17*	61	18	2550
18*	37	12	2834
19	38	15	3676
20*	100	17	3940
21	35	8	578
22	30	9	1185
23	66	9	1459
24	72	14	1573
25	67	11	2200
26*	80	17	2491
27	86	13	3379
28	87	20	3038
29	49	12	2763
30	83	8	3922
31	82	18	3629
32	74	8	4444
33	97	12	4530
34	102	6	4830
35	127	14	5639
36	107	9	6349
37	86	8	6119

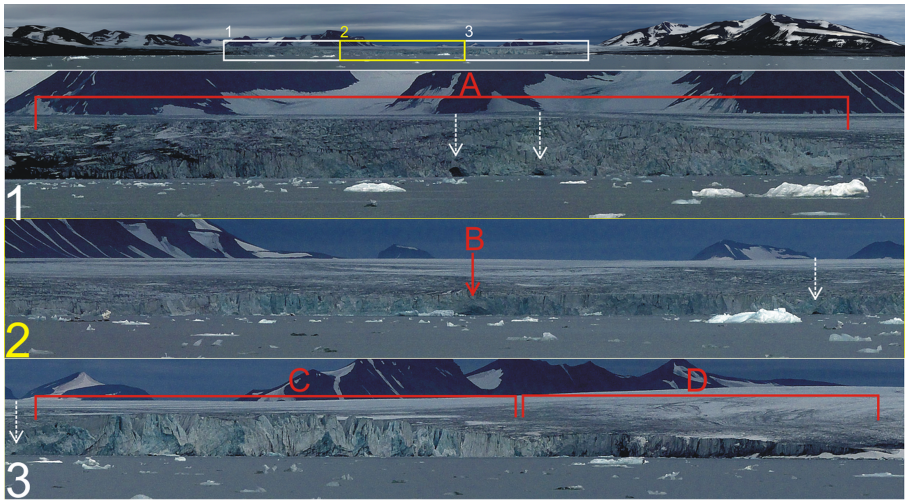

Figure 2: Photograph of Hornbreen's ice cliff taken in August 2009 (general view and detailed view of zones distinguished within the ice cliff: A – strongly crevassed zone, B – main meltwater outflow zone, C – high cliff zone and D – permanently bay-shaped zone). Tidewater caves are marked with white dashed arrows.

with diameters smaller than 0.5 mm was performed using laser particle-size analyser (Analysette 22 Comfort Fritsch). Time of ultrasonic disintegration was 2–3 minutes and the amount of sediment in measurement cell was 9–17%. The main reason for using the boundary value of grains' diameter equal 0.5 mm was relatively small mass of analysed samples, what would have resulted in small accuracy of very fine – medium sand content measurement. The results of grain-size analyses are presented as weight (fraction >0.5 mm) and volume (fraction <0.5 mm) percentages in the form of frequency curves (Figures 4, 5). Additionally, cumulative histograms presenting each fraction content in every slice has been prepared (Figures 6, 7). Grain-size analysis was performed with 1-phi fraction accuracy within 2 mm–0.122 μm limits.

'Surface samples' were wet-sieved using 0.063 mm Fritsch sieve. Then sediment of the >0.063 mm fraction was dry-sieved using 0.122 mm, 0.250 mm, 0.500 mm, 0.930 mm and 2 mm sieves. Analysis of fractions <0.063 mm was performed using laser particle-size analyser (Analysette 22 Comfort Fritsch). The results are presented as weight (fraction >0.063 mm) and volume (fraction <0.063 mm) percentages in the form of frequency curves (Figure 8). Grain-size analysis was performed similarly, with 1-phi fraction accuracy within 2 mm–0.122 μm limits.

In both cases, grain-size parameters (mean diameter, sorting, skewness and kurtosis) were calculated using GRADISTAT 4.0 [22]. For the purpose of interpretation, logarithmic (original) Folk and Ward (1957) graphical measures were used. Grain-size fractions' limits were determined according to modified Udden – Wentworth grade scale adopted in GRADISTAT [22]. For description of sediments major textural groups and detailed sediment names after Folk (1954) were used [22, 23].

The maps of each fraction content and grain-size parameters' distributions in the entire survey area were created using Natural Neighbour interpolation method (Figures 9, 10, 11). In order to provide reliable data, weighted average of each fraction content in three surface slices of 'axial cores' was calculated.

4 Results

Hydrography. Hydrological conditions in proximity of Hornbreen ice cliff can be described on the basis of CTD and current profiles collected at point C1. The obtained results show a distinct temperature-salinity stratification of water column (Figure 3A). Existence of four main water layers has been stated: surface layer of cool brackish water at depth 0–11 m originating from glacier melting (1), layer of water mixing (depth 11–25 m), where rapid changes of temperature and salinity occur (2), layer of fjord water (depth 25–50 m) with a regular increase of density and salinity, and decrease of temperature in term of depth (3), layer of over-cooled dense water (depth 50–55 m) remained from winter mixing (4). Existence of the latter even during late summer seasons in 1999, 2000 and 2002 has also been proved [24]. Similar summer water column salinity stratification was observed in Brepollen in July 2002. Measurements undertaken at the distance of ca. 5 km from glaciers' fronts showed salinity increase from less than

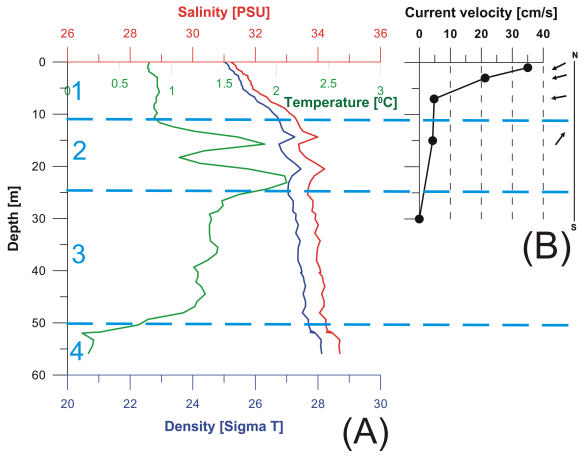

Figure 3: Water column properties obtained from (A) CTD profile and (B) current measurements at point C1. The following water layers has been distinguished (marked with blue numbers and dashed blue lines): 1 – surface layer of cool brackish water, 2 – layer of water mixing, 3 – fjord water layer, 4 – layer of over-cooled dense water remained from winter mixing.

28 PSU (Practical Salinity Units) at surface to 34.68 PSU close to the bottom (ca. 138 m below sea level) [24]. Moreover, similar results have been obtained in the forefield of Kongsbreen (Kongsfjorden, Svalbard), where the measured thickness of surface layer of brackish water, at the distance of ca. 0.45 km from the glacier's front, was ca. 10 m [25]. According to the current measurements the main water current is directed at WSW (Figure 3B). The rapid decrease of meltwater outflow velocity with depth, from 35 cm/s at 1 m below sea level (b.s.l.) to 5 cm/s at 7 m b.s.l., is observed. The existence of at least one vortex cell can be suspected at depth of 15 m, where current direction changes to opposite.

Sediment properties and grain-size distribution. Sediments collected from 'axial cores' belonged mainly to the textural group of muds, secondarily sandy muds (sediment names varied from very fine silt to coarse silt Table 2), and showed unimodal grain-size distribution in all slices (cores 8, 17, 18, 26) or unimodal and bimodal grain-size distribution (cores 4, 9, 20). The most prominent mode was in medium silt fraction (≈6.5 phi) and the secondary mode in very fine silt fraction (≈8.5 phi). Exceptions were cores 13 and 14, closest to the ice cliff, in which textural group of sandy muds was dominating (sediment names varied from fine silt to very coarse silty very fine sand – Table 2), grain-size distribution varied from unimodal to trimodal and dominating fractions were medium silt (≈6.5 phi), very fine silt (≈8.5 phi) and very fine sand (≈3.5 phi) in different combinations (Figures 4, 5). All sediments had dark greenish colour and were poorly to extremely poorly sorted, mainly with symmetrical or platykurtic grain-size distribution.

Sediments derived from 'surface samples' fell mainly into the textural group of muds, secondarily sandy muds (samples 1, 6, 21, 33), whereas sediment names varied from fine silt to very coarse sandy fine silt (Table 3). Sediments had mostly unimodal grain-size distribution with dominating fraction of fine silt (≈7.5 phi). Bimodal grain-size distribution with the second dominating fraction of very fine sand (≈3.5 phi) has been observed only in samples 1 and 21. Sediments were of dark greenish colour, poorly and very poorly sorted with mainly symmetrical grain-size distribution (Figure 8).

Sediments usually contained gravel grains interpreted as dropstones. Sands consisted mainly of mineral grains, nevertheless, skeleton fragments of foraminifera and other marine organisms did also occur.

Several important observations have been made on the basis of sediment grain-size distribution along longitudinal and transverse profiles (Figures 4, 5, 6, 7): the content of sandy and gravel fractions in cores closest to the ice cliff (13, 14) is significantly higher than in other cores (Table 4) (1), the content gravel and sands decreases with increasing distance from the ice cliff (2) and the content of gravel shows indistinct regularity in term of depth in cores 14, 4, 20 (3).

Moreover, sediment grain-size distribution in the entire survey area has been described on the basis of 'surface samples' analysis. In general, the content of sands and gravel decreases irregularly with distance from the ice cliff (Figures 9A, 9B, 9C). The area of increased gravel fraction content comprises mainly samples 13 and 14 (Figure 9B). The content of sands, however, reaches the highest value of 24.4% in sample 1 (Figures 9C). Incidentally, higher content of gravels and sands is observed in samples 6, 33 and 30, 33 respectively (Figures 9B, 9C). Grain-size distribution maps prepared only on the basis of silt and clay content reveal, that relatively higher content of clay in comparison to silt is observed along longitudinal axis of the forefield (Figures 9D, 9E). Furthermore, the content of silt fraction is higher in areas close to the valley slopes (samples 1, 2, 25, 29, 18, 19) and on the bottom elevations (samples 14, 21, 22) (Figure 9D).

Interpretation of grain-size distribution. The grain-size distribution in 'axial cores' indicate a strong disproportion between sediments in cores 13, 14 and sediments in other cores, resulting from their close proximity to the ice cliff (core 13), what means higher energy of meltwater outflow, and relatively shallow depth (core 14). Furthermore, core 14 is also under the influence of Hornbreen's high cliff zone (Figures 1A, 2), where numerous icebergs loaded with

Table 2: Sediment names determined for slices of 'axial cores' according to Folk (1954) scheme. Cores 13 and 14 with significantly high content of gravel and sands were marked with *.

Sediment depth interval	Core number								
	4	8	9	13*	14*	17	18	20	26
0—1	medium silt	-	medium silt	fine silt	very fine sandy coarse silt	-	very coarse sandy medium silt	medium silt	medium silt
1—2	coarse silt	medium silt	fine silt	medium silt	very coarse sandy medium silt	medium silt	medium silt	medium silt	medium silt
2—3	medium silt	medium silt	medium silt	very coarse sandy medium silt		medium silt	medium silt	medium silt	medium silt
3—4	very fine sandy medium silt	medium silt	medium silt	very fine sandy medium silt	medium silt	medium silt	medium silt	medium silt	medium silt
4—5	very fine silt	medium silt	very coarse sandy medium silt	very fine sandy very fine silt	very fine sandy very coarse silt	medium silt	medium silt	medium silt	medium silt
5—6	very fine silt	medium silt	medium silt	very fine sandy medium silt	very fine sandy very coarse silt	medium silt	very coarse sandy medium silt	very fine silt	medium silt

Table 2: Cont.

Sediment depth interval	Core number								
	4	8	9	13*	14*	17	18	20	26
6—7	very coarse sandy very fine silt	medium silt	medium silt	very fine sandy medium silt	very fine sandy very coarse silt	medium silt	medium silt	very fine silt	medium silt
7—8	very fine silt	medium silt	medium silt	ver fine sandy medium silt	very coarse silty very fine sand	medium silt	medium silt	very fine silt	medium silt
8—9	very fine silt	medium silt	medium silt	-	very fine sandy very coarse silt	medium silt	medium silt	medium silt	very coarse sandy medium silt
9—10	very fine silt	medium silt	-	-	very fine sandy very coarse silt	fine silt	medium silt	very fine silt	medium silt
10—11	very fine silt	medium silt	-	-	very coarse snady very fine silt	fine silt	medium silt	very fine silt	medium silt
11—12	very fine silt	fine silt	-	-	very fine sandy very coarse silt	very fine sandy medium silt		medium silt	medium silt
12—13	very fine silt	medium silt	-	-	very fine sandy very coarse silt	very fine silt	-	very fine silt	medium silt

Table 2: Cont.

Sediment depth interval	Core number								
	4	8	9	13*	14*	17	18	20	26
13—14	very fine silt	coarse silt	-	-	very fine sandy very fine silt	very fine silt	-	very fine silt	medium silt
14—15	very fine silt	medium silt	-	-	-	very fine silt	-	medium silt	medium silt
15—16	very fine silt	medium silt	-	-	-	very fine silt	-	medium silt	very coarse sandy medium silt
16—17	-	very coarse sandy medium silt	-	-	-	very fine silt	-	medium silt	medium silt
17—18	-	medium silt	-	-	-	medium silt	-	medium silt	-
18—19	-	medium silt	-	-	-	-	-	-	-
19—20	-	medium silt	-	-	-	-	-	-	-
20—21	-	medium silt	-	-	-	-	-	-	-
21—22	-	medium silt	-	-	-	-	-	-	-
22—23	-	medium silt	-	-	-	-	-	-	-

Table 3: Sediment names determined for 'surface samples' according to Folk (1954) scheme.

'Surface sample' number	Sediment name
1	very fine sandy fine silt
2	fine silt
3	fine silt
5	fine silt
6	very coarse sandy fine silt
7	fine silt
10	fine silt
16	fine silt
19	fine silt
21	very fine sandy fine silt
22	fine silt
23	fine silt
24	fine silt
25	fine silt
27	fine silt
28	fine silt
29	fine silt
30	fine silt
31	fine silt
32	fine silt
33	very coarse sandy fine silt
34	fine silt
35	fine silt
36	fine silt
37	fine silt

Table 4: Weighted average content of gravel and sands in 'axial cores'. Cores 13 and 14 with significantly high content of gravel and sands were marked with blue colour.

Core number	Average gravel content [%]	Average sands content [%]
4	3.09	2.33
8	1.55	1.1
9	3.84	0.53
13	6.02	14.81
14	8.32	24.64
17	1.16	4.51
18	4.52	3.23
20	1.11	1.08
26	4.46	3.46

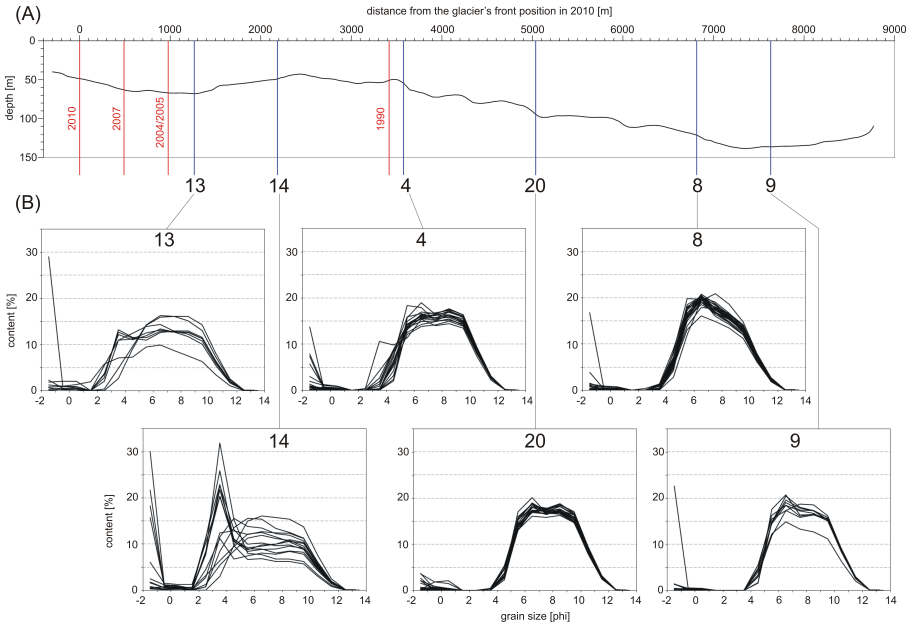

Figure 4: Sediment distribution along longitudinal profile at Hornbreen's forefield. (A) Sea bed morphology along the profile. Blue lines indicate localizations of 'axial cores', red lines positions of the ice cliff in given years. (B) Frequency curves of sediments obtained from separate slices of each 'axial core'.

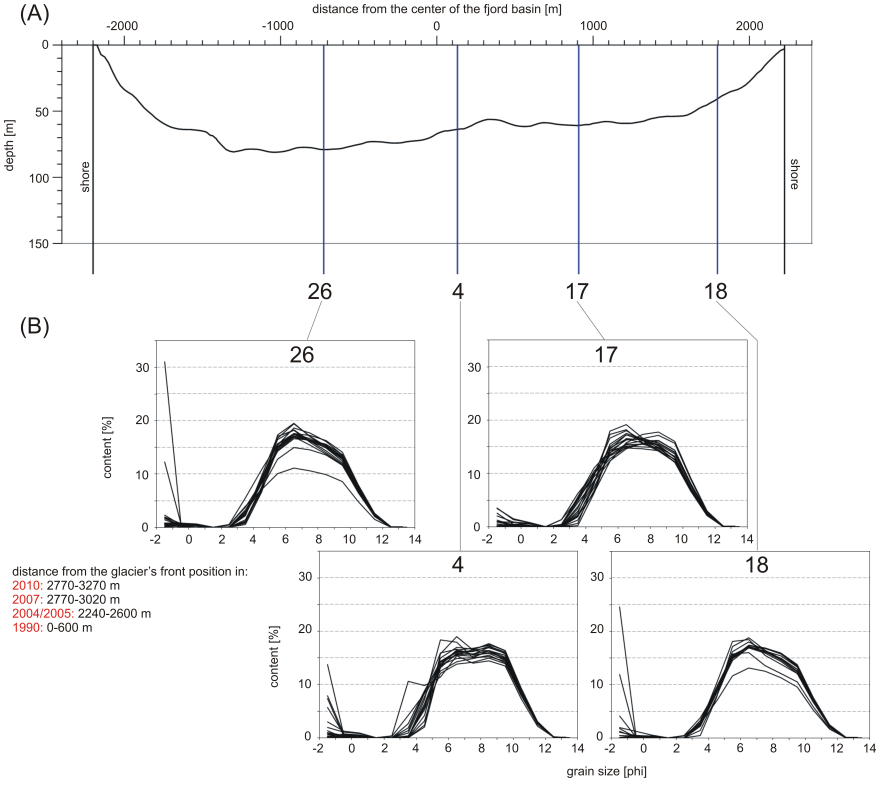

Figure 5: Sediment distribution along transverse profile at Hornbreen's forefield. (A) Sea bed morphology along the profile. Blue lines indicate localizations of 'axial cores'. The shores are marked with black lines. (B) Frequency curves of sediments obtained from separate slices of each 'axial core'.

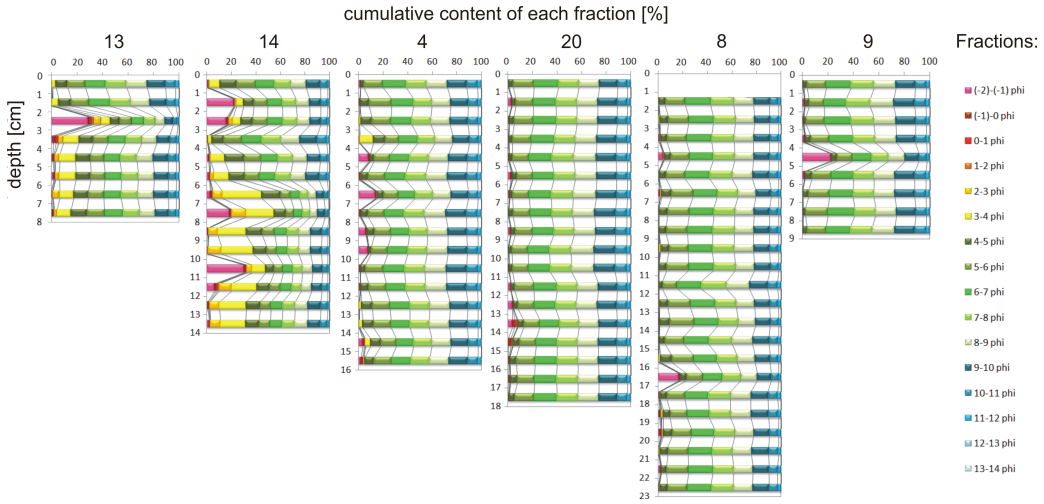

Figure 6: Cumulative histograms of each fraction content in sediments obtained from slices of 'axial cores' situated along longitudinal profile of Hornbreen's forefield.

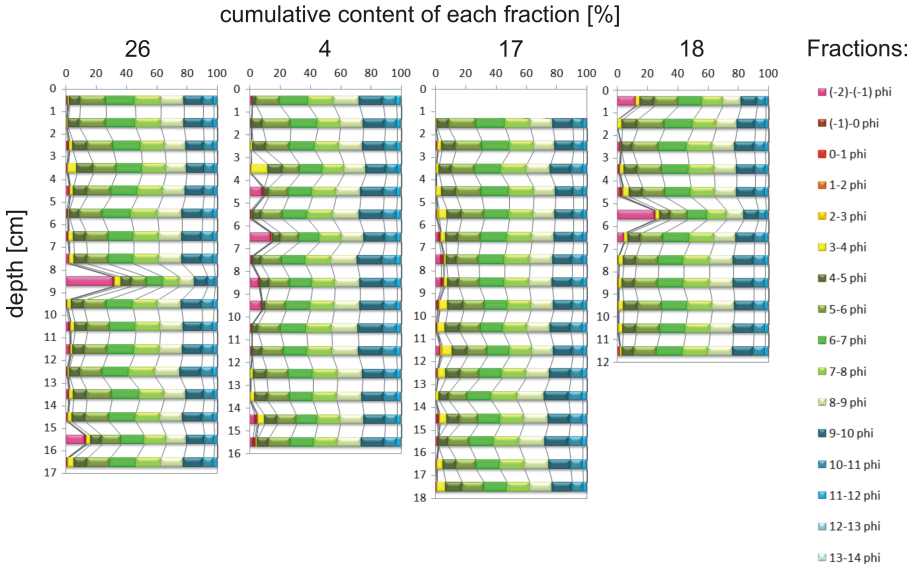

Figure 7: Cumulative histograms of each fraction content in sediments obtained from slices of 'axial cores' situated along transverse profile of Hornbreen's forefield.

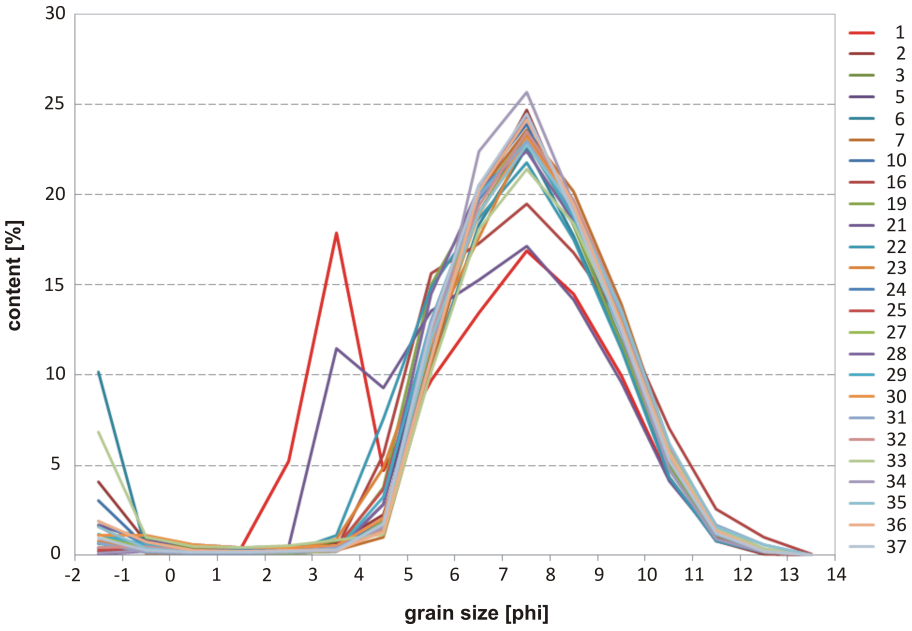

Figure 8: Frequency curves of sediments obtained from 'surface samples'. In the legend 'surface samples' numbers are listed.

sediment are produced (Figure 12). Rapid increase of very fine sand content at depth of 6 cm in core 14 could be an image of the cliff's past position which led to formation of morainal bank or recessional moraine (Figure 6). The regularity in incidental appearance of gravel in analysed cores is a result of intensified glacier calving and, therefore, icebergs' drifting and melting during summer season. Intensity of these processes seems to be decreasing with distance.

The decrease of sands and gravels content described on the basis grain-size distribution in 'surface samples' is partly an image of declining energy of meltwater outflow with increasing distance from the ice cliff [10, 11, 27]. The tendency is clearly visible to the distance of about 2.5 km from the cliff (Figure 9A, Table 1). Further, the grain-size distribution is less diverse due to the continuous and gradual suspension settling of the finest particles (Figure 10A), however, sediments are still becoming finer with increasing distance from the ice cliff (Figure 11A). Here and there coarser grains melted out from drifting icebergs are observed (samples 6, 30, 33) (Figures 9A, 10A, 12). Increased content of gravel in samples 13 and 14 is probably a result of intensified icebergs' activity or formation of accumulative forms, such as morainal banks or submarine outwash, in the marginal zone [26]. Additionally, the existence of dynamic outflow or occurrence of gravity flows from the fjord slope could be suspected in the region of sample 1 (Figure 12), due to its highest sands content. The probable occurrence of gravity flows is also reflected in the distribution of silt, which tends to accumulate close to the valley slopes. Predominance of silt over clay fraction on bottom elevations is a result of intensified current reworking and iceberg scouring (Figure 12). It is worth mentioning, that the area of increased sands content, extending along samples 1, 2, 24 and 25, is a result of interpolation algorithm behaviour (Figure 9C).

Controls on diversity of grain-size statistical parameters. The results of grain-size statistical parameters' distribution analysis reveal irregular decrease of the mean diameter of grains (GSS) with increasing distance from the ice cliff and from SE shore (Figures 10A, 11A). Such distribution of GSS confirms the fact of environment energy decrease with increasing distance from the ice cliff. The main transport of sediment occurs along the longitudinal axis of the forefield from the glacier's ice cliff to central Brepollen (Figure 10A), mainly in the meltwater plume, what is characteristic for all Spitsbergen glacier-influenced fjords [27]. According to GSS distribution map, the secondary sources of sediment are the shores of peninsulas restricting Hornbreen from N and S, from which moraine material is transported by seasonal streams (1) and valley slopes which are the source of submarine slides and gravity flows (2) (Figures 10A, 12). Moreover, relatively low value of GSS in SE part of the forefield (samples 14, 21, 22) indicates intensified current reworking and iceberg scouring on this bottom elevation (Figures 10A, 11A, 12). Positive anomalies in GSS distribution observed in samples 6, 8, 26 and 33 are an effect of ice-rafted debris sedimentation, so no sediment transport directions were determined on the basis of them (Figure 10A). The sediment sorting coefficient

(GSO) decreases irregularly with increasing distance from the cliff (Figures 10B, 11B) and worse sorting of silt and clay fractions was identified in SE part of the forefield than in its NW part (Figure 11B). The poor level of sorting in analysed sediments is an effect of superposition of different deposition processes and seasonal changes of environment energy. On the basis of GSO distribution it could be appointed, that the highest diversity of depositional processes occurs in close proximity to the ice cliff (the area of samples 13 and 14), where the level of sediment sorting is the lowest. Further from the cliff, where gradual suspension settling dominates and sedimentation becomes more calm and homogenous, observed sediment sorting level increases (Figure 10B). The probable reasons for relatively low GSO value in the area of samples 2, 3 and 24 (Figure 11B) are: the transport of deposits from the shore by seasonal streams, which energy condition the size of particles that can be carried out (1) and northern deflection of the outflow, which could dominate other sediment sources in this region (Figure 12). Furthermore, gradual change of sediment skewness (GSK) from coarse skewed in the proximity of ice cliff to symmetrical in central Brepollen has been observed (Figures 10C, 11C). This trend simply reflects the fact, that coarse fractions (sands and gravel) are deposited close to the glacier terminus, whereas grains of silt and clay fractions are transported to the central part of Brepollen in the meltwater plume. Moreover, relatively low value of GSK is visible in the area of samples 14, 21 and 22 (Figure 11C). The observed anomaly is probably a result of intensified sediment winnowing and reworking, described earlier on this bottom elevation on the basis of GSS distribution. However, negative values of GSK could be also a result of active redeposition processes [28], which probably occur in this region in the form of slides, gravity flows and iceberg scouring (Figure 12). Finally, relatively high values of kurtosis (GSP) are observed in the proximity of the glacier terminus, where sample 2 reveals even very leptokurtic grain-size distribution (Figure 10D). The anomaly is related to the very high content of fine silt (24.7%) in sample 2 and neighbouring samples 3, 23 and 24. According to [28], such domination of one fraction is an indicator of homogenous and dynamically unstable conditions, which could be an effect of activity of a current process, such as dynamic outflow. This supposition could be confirmed by relatively low GSO values occurring in this region. Additionally, the map calculated only on the basis of silt and clay fractions' content show that GSP values are higher in the SE part of the forefield than in its NW part (Figure 11D), what is probably connected with winnowing of clay fraction from bottom elevation. Generally, platy- and mezokurtic grain-size distributions, which dominate in the survey area, indicate that the amount of sediment is typical for analysed sedimentary system or even bigger [28]. Local disturbances of GSS, GSO, GSK and GSP distributions occur in cores 33 and 6, due to sedimentation of ice-rafted debris (IRD). It has been noted that the maps of grain-size parameters prepared for all fractions provide information concerning the influence of the glacier on sediment distribution (Figures 10A, 10B, 10C), whereas the maps of parameters calculated only on the basis of silt and clay content reveal also the relation between sediment properties and bathymetry (Figures 1B, 11A, 11B, 11C).

5 Discussion

Glacier-influenced fjords are considered to be a low-energy basins which are effective traps for sediment. Most of the sediment is deposited near the ice terminus and intensity of sedimentary processes decreases rapidly away from the ice margin [10, 11, 25]. According to [10], four main sets of processes distributing sediments in glacier-influenced fjords are: ice-contact processes that control the release of sediments (1), fluvial processes that transport sediments through the fjord (2), icebergs and sea ice rafting (3) and deep-water currents (4). Subsequently, deposits may be redistributed by secondary processes, such as gravity flows, slides or wave and tidal action. Generally, meltwater discharge and iceberg calving are considered to be the most effective processes influencing sediment distribution and overwhelming the impact of ice-front melting [10, 26]. Depending on the climate conditions, the relation between the influence of meltwater and the influence of ice-related processes change [27]. High air and water temperatures result in the big amount of meltwater produced, what can be widely observed in temperate fjords (e.g. Alaskan), where glacimarine sedimentation is dominated by meltwater processes [27, 29, 30]. On the other hand, in colder settings, such as East Greenland or Antarctica, iceberg sedimentation becomes more important [27, 31, 32]. Particularly, in the fjords of Spitsbergen the influence of meltwater has been proved to be dominating [27, 33, 34]. This thesis has been confirmed by the research undertaken in glacier-influenced Kongsfjorden (Spitsbergen), where the main sediment transporting factor is buoyant hypopycnal flow of brackish water originating from big englacial tunnel [25, 33]. However, it has also been proved that fjords of Svalbard, where mainly polythermal glaciers occur, are less strongly influenced by meltwater sediment delivery than temperate fjords are [35].

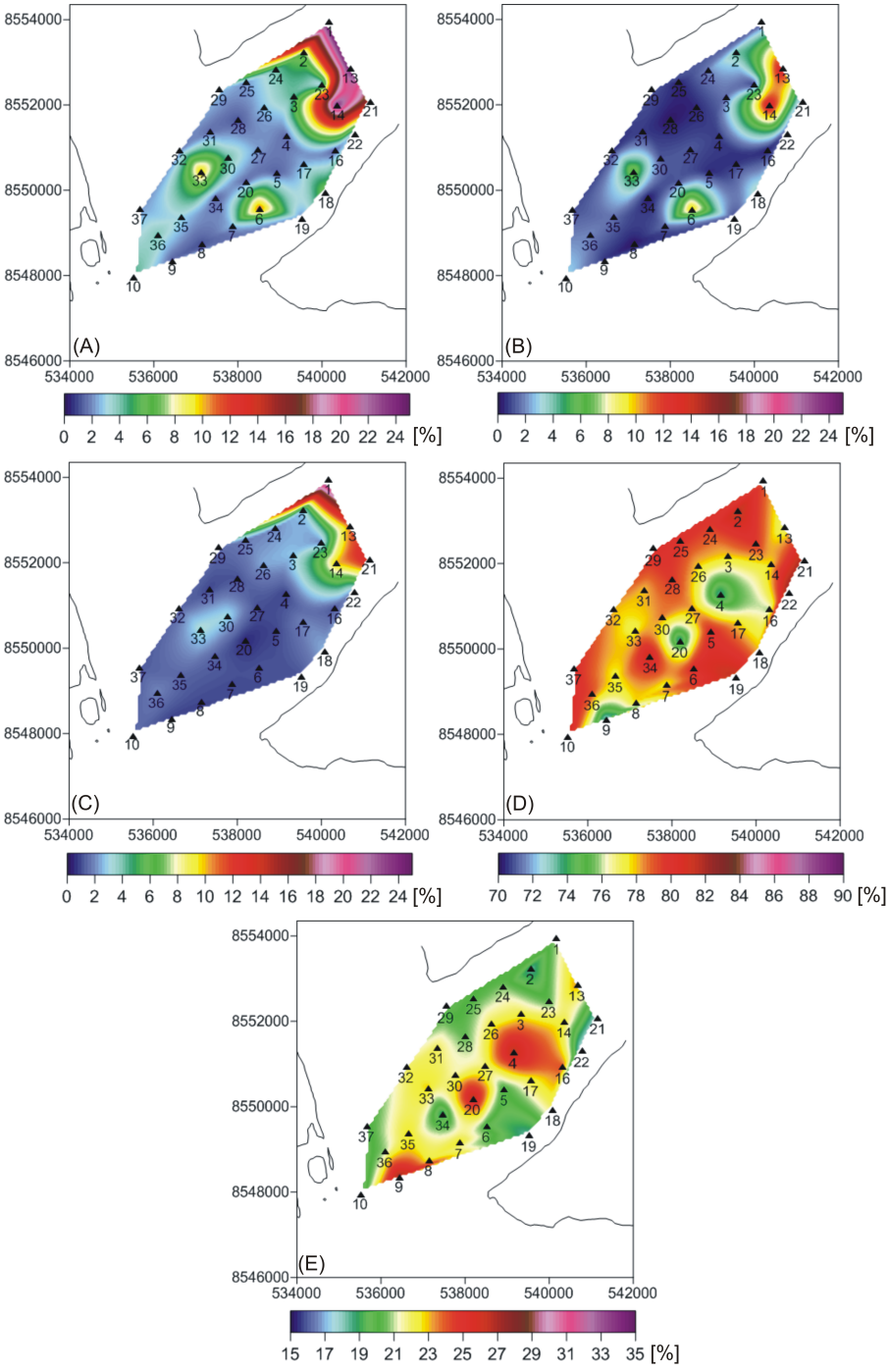

Figure 9: Maps of sediment grain-size distribution: (A) gravel and sands content, (B) gravel content, (C) sands content, (D) silt content after recalculation of silt and clay fractions to 100%, (E) clay content after recalculation of silt and clay fractions to 100%. All fractions contents are given in percentages.

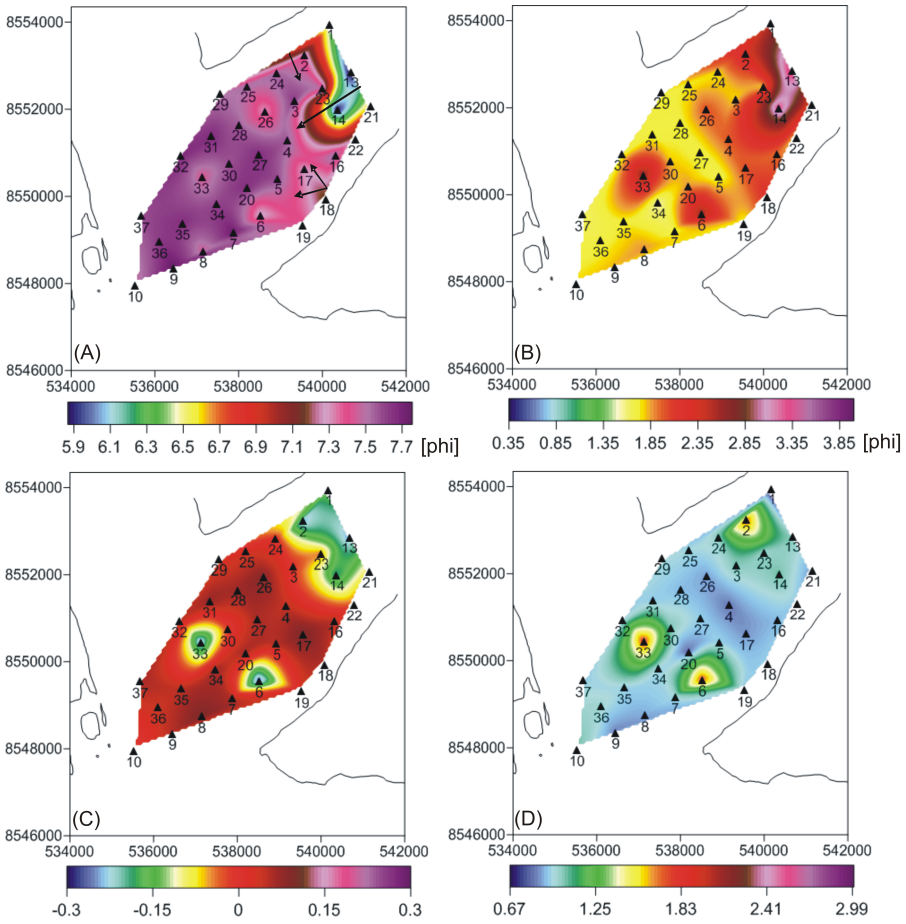

Figure 10: Maps of sediment grain-size parameters' distributions: (A) mean diameter (GSS), (B) sorting (GSO), (C) skewness (GSK), (D) kurtosis (GSP). Parameters' values were calculated from all fractions. In Figure 10A main transport directions, determined on the basis of particles' mean diameter (GSS) distribution, are marked with black arrows.

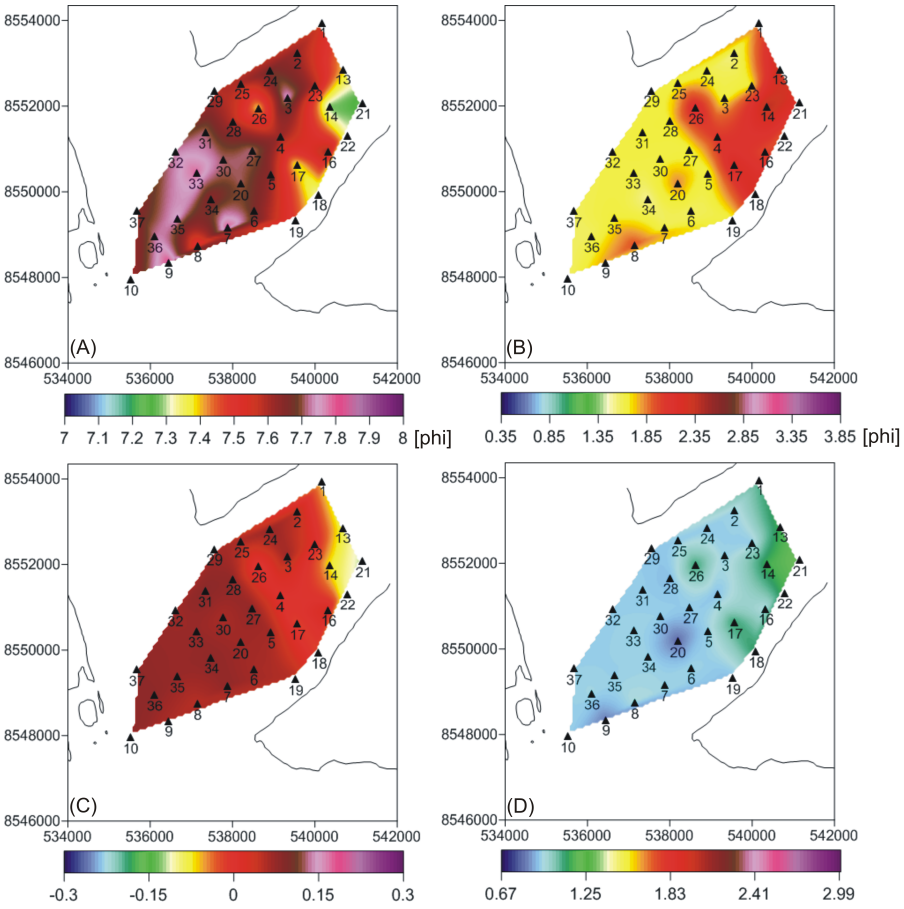

Figure 11: Maps of sediment grain-size parameters' distributions: (A) mean diameter (GSS), (B) sorting (GSO), (C) skewness (GSK), (D) kurtosis (GSP). Parameters' values were calculated only from silt and clay fractions.

Sedimentary processes in glaciomarine environments are complicated and depend on numerous factors, such as bathymetry, salinity, marine currents and tides or seasonal temperature changes. Therefore, detailed analysis of sedimentation in front of a tidewater glacier requires complex measurements of water column properties, currents and suspension load which have not been undertaken in this research. Nevertheless, on the basis of information gathered about Hornbreen and sediments' grain-size distribution in its forefield, the general description of depositional processes in this area has been given.

Ice-contact processes. In case of Hornbreen direct deposition from the ice cliff, comprising dumping or release of supraglacial and englacial debris by melting at the ice margin [9], is not possible to determine, because the nearest sampling station (1) is located at the distance of ca. 426 m from the cliff, whereas ice-contact processes cause most sediment to be deposited very close to the ice terminus [10]. However, this type of sedimentation needs to occur due to englacial and supraglacial debris content, glacier's regular movement and temperature difference between ice and water (Figure 12) [10]. The good evidence of this process are recessional moraines visible on the Hornbreen's forefield bathymetric map [14, 36].

Meltwater outflow. On the contrary, glaciofluvial processes which comprise deposition from meltwater flows and settling from suspension, have a visible influence on sediment distribution in the study area. On the basis of photographic documentation of Hornbreen's cliff, existence of at least five probable tidewater caves in its NW part can be determined (Figure 2). These tidewater caves are good indicators of localization of discharge outlets functional in recent past [10]. Moreover, a form of calving bay in the central part of Hornbreen's cliff is visible among at least the last three years (Figure 1A). The bay is considered to be a result of activity of the biggest present meltwater discharge. Another indicator of this outflow is a big tidewater cave located in this area (Figure 2). The current measurements undertaken at point C1 (Figure 1A), exactly in the axis of main meltwater outflow, were used to determine exact position of the tunnel outlet. It turned out to be situated in the centre of the bay (Figure 12). The current velocity decrease with depth indicates, that at the distance of about 393 m from the ice cliff, the submarine discharge jet has reached sea level and is propagating as surface buoyant plume. As sedimentation of jet suspended load peaks at the position, where the jet begins to rise from the level of discharge outlet [10], none of the collected cores can reflect these conditions with reference to analysed outflow. The sediment particles fallout progressively from the jet, due to the velocity and jet momentum decay according to Stokes' law [10, 25]. According to [10], about 70% of the sediment load is deposited within the first 500 m from the ice front. The research undertaken in Kongsfjorden indicates, that even ca. 90% of total sediment input is deposited within distance of 400 m from the ice cliff [37]. The other type of submarine discharge that should be considered is underflow which occurs in case of exceptionally high concentration of sediment load in the efflux. However, such concentrations are considered to be seldom in present glacier-influenced fjords [10], so they will not be taken into account in the case of Hornbreen. There is no information concerning supraglacial discharge, though it probably becomes part of englacial discharge due to the presence of numerous crevasses in the glacier close to the ice front position. It is worth mentioning, that in case of subglacial discharge occurrence bedload is deposited directly at the discharge outlet in the form of grounding line fan, from which material is redistributed by sediment gravity flows [9, 26, 27]. In Spitsbergen fjords submarine fans are often well developed [27].

The sediment distribution feature that could reflect existence of submarine, even subglacial, discharges from Hornbreen's ice cliff is the higher content of gravels and sands in sample 13 which is located on the axis of main meltwater outflow. On the contrary, even higher content of these fractions in sample 14 must be related to other sedimentary processes, due to its bigger distance from the ice cliff and southern deflection from the axis of the outflow. The probable reasons for this anomalous distribution will be discussed in further part of the paper. The highest content of sands in sample 1 (22.4%) could also be a result of submarine discharge activity, as the existence of several tidewater caves in NW part of the cliff implies (Figure 2).

Settling from suspension. Glacier-influenced fjords are settings, where fine-grained sediments (silt and clay) tend to dominate [27]. The smallest particles which were not deposited during rising of the meltwater discharge, are transported downward the fjord in the overflow plume [38]. The distance the particle is carried away depends directly on the surface plume velocity and on the time it can remain in surface layer [10]. Indirectly, this distance varies due to freshwater discharge, basin morphology and external forces, such as tides and winds. After leaving the surface layer the particle is starting its residual descent vertical path. Settling of particles proceeds gradually according to Stokes' law, however, processes such as flocculation, agglomeration or pelletisation accelerate deposition of joined particles [9, 10, 38]. The plume can transport in suspension the particles up to fine sand fraction [38]. In the Hornbreen's forefield the process of gradual suspension settling is reflected as regular decrease of the mean

diameter of grains (GSS) with increasing distance from the ice cliff (Figures 10A, 11A).

Iceberg calving. As mentioned earlier, iceberg calving is generally an important factor controlling sediment distribution in glacial-influenced settings, however, not the one of the biggest importance in fjords of Svalbard. Ice-rafted component of bottom sediments has been mentioned as the one of even minor significance in Kongsfjorden [33]. In the Hornbreen's forefield the influence of icebergs' activity on sediment distribution has been observed. It has been estimated that iceberg calving contributes 17–25% of total mass loss of Svalbard glaciers', with the average value of 21% [1]. In case of Hornbreen estimated calving intensity equals 0.0271 $km^3 a^{-1}$ [1]. In general, four types of icebergs, depending on their genesis and ability to release sediment, has been described [10]. The icebergs originating from subaerial jointing of ice blocks and jointing of ice blocks around ice caves or along tidewater indenture, tend to lose their material immediately near the ice front through iceberg overturning and plunging, whereas large icebergs (mega-icebergs) formed by detachment along crevasse system transport sediment to the mouth of the fjord by rafting. In the case of Hornbreen, the zone of strongly crevassed high cliff (Figures 1A, 2) is the origin of mega-icebergs, whereas in the NW part of the cliff icebergs originating from caves are more likely to occur. The height of Hornbreen's ice cliff, estimated to about 70 m a.s.l. in 2000 [4], enables jointing of icebergs of similar size. It means that in SE part of the forefield, where bottom elevation of about 35 m b.s.l. is observed (samples 21, 22, 14), mega-icebergs can cause reworking of bottom sediments creating forms, such as plough marks, grooves, sprag and jigger marks or gravity craters [9]. In Hornsund the greatest icebergs could reach ca. 25 m high, what means that the depth of bottom sediment penetration is several times greater [11]. Moreover, icebergs frequently remain jammed in NE and SW parts of Brepollen [11]. Nevertheless, according to [13], iceberg-caused sediment reworking in the fjord occurs mainly to the depth of 20 m and at greater depths it is less pronounced.

Bottom sediments reworking by mega-icebergs in SE part of Hornbreen's forefield (high cliff zone) is one of the probable reasons for abnormally high content of coarse fractions in sample 14. Additionally, intensified sediment melting out from drifting icebergs should be taken into account, due to their tendency to accumulate in this region (Figure 12). The activity of icebergs is clearly visible on sediment distribution maps as high content of gravels (samples 33, 6) and sands content anomalies (samples 30, 33) at big distances from the ice cliff, due to sedimentation of ice-rafted debris (IRD). As mentioned earlier, regularity in incidental appearance of gravels (Figure 6) is a result of intensified glacier calving and, therefore, icebergs drifting and melting during summer season.

The sedimentary processes described above are responsible for the primary accumulation of sediments in the glacier's forefield. However, for detailed analysis of the entire glaciomarine sedimentary system, secondary processes, such as redepositional ones, should be taken into consideration.

Redepositional processes. Redeposition of sediments in glacier-influenced fjords is a result of tides and waves action and slope instabilities [10]. In Brepollen region tidal currents probably do not affect sediment distribution significantly, because of its internal localization and generally low tide amplitude in Hornsund (up to 1.5 m) [11]. On the contrary, the influence of current reworking on sediment distribution has been proved to be significant in Kongsfjorden, where generally coarser sediments are observed on the slopes and sills than inside the basin [33]. The sediment reworking can be also caused by deep water renewal events, which take place only in the years of abnormally strong inflows of Atlantic Core Water into the fjord [39]. In such situations dense cold bottom water, formed during winter freezing, is exchanged with the outer fjord water masses [11].

According to [10], there are three types of waves that can cause sediment redeposition: surface waves created by diurnal land-sea breezes and storm winds, iceberg calving generated waves and giant waves resulting from earthquakes and subaerial debris dislodging from fjord margins. Generally, the height of waves seldom exceeds 3 m in most fjords, what implies wave base not deeper than 20 m b.s.l. [10]. Therefore, this type of waves cannot have a significant impact on sediments redistribution. Svalbard region is generally described as seismically active area [40], with most of strong earthquakes occurring along the Mon and Knipovitch Ridges and the Storfjord Channel, which is located on the east side of Spitsbergen at nearly the same latitude as Brepollen. The strong events, which occur there in intervals of several years, are usually followed by series of aftershocks [40]. Therefore, the influence of earthquakes on slopes' stability and creation of giant waves should not be neglected. However, among all the other wave types probably the iceberg calving generated waves would be the ones of the biggest importance for sediment redeposition in Hornbreen's forefield.

Unfortunately, the impact of currents and waves action on sediment distribution in the forefield of Hornbreen is not possible to determine on the basis of available data. For this purpose more data concerning water column properties and calving intensity should be collected.

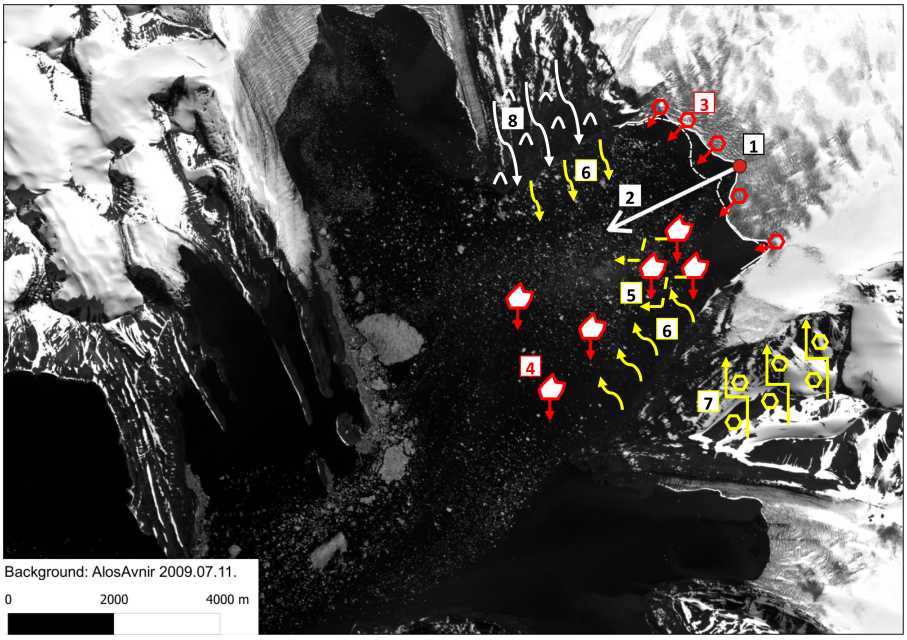

Figure 12: The scheme of sedimentary processes: 2 – deposition from meltwater discharge (deposition of coarse-grained bed load and slow sedimentation of fine-grained sediments from meltwater plume), 3 – direct deposition from the ice cliff (dumping and release of supraglacial and englacial debris by melting), 4 – deposition from icebergs, 5 – redeposition of sediments by iceberg scouring, 6 – redeposition of sediments by slides and gravity flows, 7 – transport of loose rock material from slopes of Ostrogradskifjella to the glacier surface, 8 – transport of moraine deposits from the shore by seasonal streams. White dashed line indicates ice cliff position in 2007 and the white solid one ice cliff position in 2009. Assumed localization of main meltwater outflow is indicated by red dot and numbered as 1.

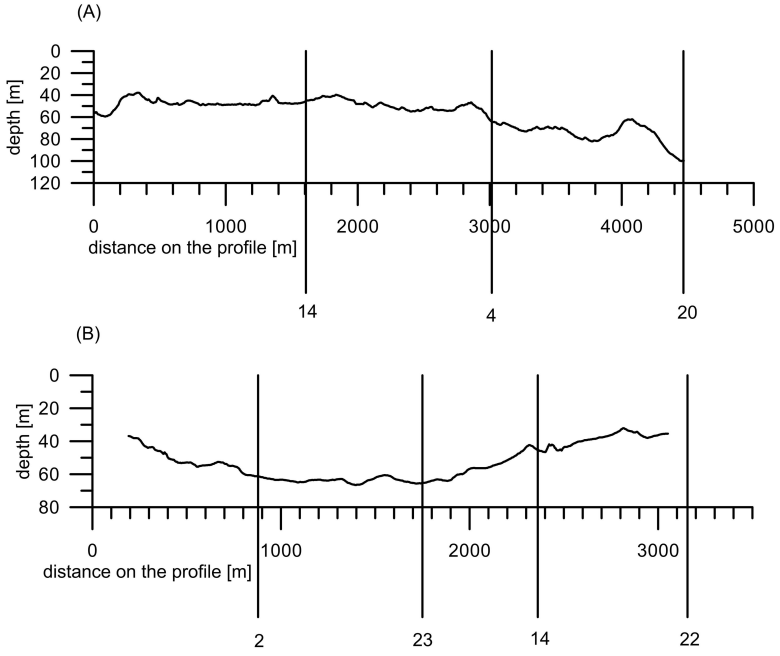

Figure 13: (A) Longitudinal and (B) transverse bathymetric profiles across sample 14 [36].

Redepositional processes, the effects of which can be observed on sediment distribution, are also slides, gravity flows and sediment creep [33, 34]. Frequency and intensity of slides, which could initiate gravity flows, depend on the fjord morphology, mainly slope steepness and relief, and sediment thickness [41]. Gravity flows are also associated with glaciomarine accumulative forms created by glacier's activity and sediment release, such as morainal banks or recessional moraines. Most of them occur within the marginal zone, where exceptionally high sedimentation rates lead to oversteepening of local slopes [10, 26, 37, 42]. Moreover, as the main reason for the occurrence of gravity flows in temperate fjords iceberg calving has also been mentioned [26]. The influence of slides, slumps, gravity flows and sediment creep on sediment distribution has been observed in Kongsfjorden [33, 37].

The analysis of cores' positions with reference to submarine landforms' locations on the basis of detailed swath-bathymetric map gives additional possible explanations for grain-size distribution anomalies [36]. In the forefield of Hornbreen were identified: recessional moraines (annual push moraines according to the nomenclature of [43]), glacial lineations and crag-and-tail structures [14]. The possible influence of these on sediment distribution will be described on the example of sample 14, which position on transverse and longitudinal bathymetric profiles has been analysed (Figure 13). Transverse bathymetric profile including samples 22, 14, 23 and 2 reveals, that sample 14 is situated between two accumulative forms of ca. 5 m height, separated by the distance of ca. 110 m (Figure 13B). According to [43], these relations suggest that, depending on their orientation which is not clearly visible on bathymetric map, the forms could be glacial lineations formed subglacially during rapid advance or rhombohedral ridges formed during post-surge stagnation. Described localization of sample 14, which favours the occurrence of mass-flow processes from both sides, is therefore one of the possible explanations for its abnormally high content of coarse fractions (Figure 9A). Similar effect can be observed in the case of sample 1, which has the highest sand content (Figure 9C). The sample is located between two glacial lineations and in close proximity of the steep valley slope, what increases the possibility of sediment redeposition. However, in this case, the proximity of the ice cliff could be also the reason for such particles' distribution. Additionally, the longitudinal bathymetric profile across sample 14 (Figure 13A) reveals the existence of at least one large transverse ridge, which could be interpreted as recessional moraine [43]. None sediment samples are located on this form. The presence of coarser deposits on valley slopes (Figure 10A) can be interpreted as a result of current reworking and sediment creep, which occur commonly in Kongsfjorden [33].

6 Conclusions

Investigations of sediment properties and its distribution in the forefield of Hornbreen revealed that the majority of modern glaciomarine sediments in this region consists of poorly sorted and extremely poorly sorted muds (according to textural groups' classification after Folk (1954)) with dominant fraction of fine or medium silt. However, sediments closest to the head of the glacier belong mainly to the textural group of sandy muds with higher content of very fine sand and polymodal grain-size distribution. As one can conclude, the sediment distribution described in the forefield of Hornbreen is generally consistent with theoretical glaciomarine models, which define ice-proximal deposits as rhythmically laminated sediments consisting of graded sand-clay couplets (cyclopsams) or graded silt-clay couplets (cyclopels) and ice-distal deposits as homogenous muds with low content of ice-rafted debris [9, 11, 26, 34]. Unfortunately, the probable lamination of ice-proximal deposits could not be observed due to the chosen core acquisition method. Nevertheless, the differences in sediments' mean grain-size between ice-proximal cores (e.g. 13 and 14) and ice-distal cores (e.g. 8 and 9) are clearly visible. It has been concluded, that the main origin of sediment material is the tidewater glacier. Sediment distribution is controlled predominantly by meltwater discharge, what is reflected as strong decreasing trend of particles' diameters with increasing distance from the ice cliff. Other sedimentary processes that influence sediment distribution are deposition from icebergs, due to the presence of IRD in sediments, and redepositional processes, such as iceberg-caused reworking, slides and gravity flows. Sediment distribution reflects seasonal changes in iceberg calving intensity and decrease of iceberg-originating sedimentation with increasing distance from the cliff. Additionally, the particles are transported from the shores of peninsulas restricting Hornbreen from N and S and from the valley slopes. These conclusions correspond perfectly with the thesis maintaining, that the dominant sediment transportation factor in subpolar fjords is meltwater outflow, which overwhelms the role of icebergs [27]. Proposed sedimentation scheme is typical for fjords of Svalbard and shows good consistency with the models suggested in papers mentioned above [25, 27, 33, 34, 37]. A novel aspect, that has not been considered in the literature, is the significance of shores as secondary sediment sources. More de-

tailed and versatile model of sedimentation in Hornbreen's forefield could be prepared only when measurements of water column properties, sediment load and accumulation rate would be carried out.

Acknowledgement: The authors would like to thank Mr Marek Zajączkowski, PhD and the staff of the Polish Polar Station Hornsund for practical assistance in field measurements and samples' collecting. Great thanks to Mr Stanisław Leszczyński, PhD and Mr Witold Szczuciński, PhD for their support in considering the matter on its merits. We are grateful to two anonymous reviewers for their critical comments on an eariler versions of the manuscript and suggestions which improved it. The project was supported by Grant No. N N525 350038 and the statutory activites no 3841/E-41/S/2015 of the Ministry of Sciences and Higher Education of Poland.
M.S. and M.M. work with data interpretation, M.S. wrote this manuscript and made all labolatory investigation. M.M. made all field measurements.

References

[1] Błaszczyk M., Jania J.A., Hagen J.O., Tidewater glaciers of Svalbard: Recent changes and estimates of calving fluxes. Pol. Polar Res., 2009, 30, 85–142.
[2] Błaszczyk M., Jania J.A., Kolondra L., Fluctuations of tidewater glaciers in Hornsund Fjord (Southern Svalbard) since the beginning of the 20th century. Pol. Polar Res., 2013, 34, 327–352.
[3] Głowacki P., Jania J.A., Nature of rapid response of glaciers to climate warming in Southern Spitsbergen, Svalbard. The First International Symposium on the Arctic Research, Drastic Change under Global Warming, Tokyo, Japan, 4-6 November, 2008.
[4] Pälli A., Moore J.C., Jania J.A., Głowacki P., Glacier changes in southern Spitsbergen, Svalbard, 1901 – 2000. Ann. Glaciol., 2003, 37, 219 – 225.
[5] Król M., Grze's M., Sobota I., Ćmielewski M., Jaworski T., Submarine evidence of the late Weichselian maximum extent and the Little Ice Age (LIA) glacier limits in the St. Jonsfjorden region (Svalbard). Bulletin of Geography - Physical Geography Series, 2010, 3, 87–102.
[6] Grze's M., Król M., Sobota I., Submarine evidence for the Aavatsmark and Dahl Glaciers fluctuations in the Kaffiøyra region, NW Spitsbergen. Pol. Polar Res., 2009, 2, 143–160.
[7] Szczuciński W., Zajączkowski M., Scholten J., Sediment accumulation rates in subpolar fjords – Impact of post-Little Ice Age glaciers retreat, Billefjorden, Svalbard. Estuar. Coast. Shelf S., 2009, 85, 345–356.
[8] Miller J.M.G., Glacial Sediments. In: Reading H.G. (Ed.), Sedimentary Environments: Processes, Facies and Stratigraphy. Blackwell Science Limited, Oxford, 1996, 454–484.
[9] Bennett M.R., Glasser N.F., Glacial Geology: ice sheet and landforms. Wiley-Blackwell, Oxford, 2009.
[10] Syvitski J.P.M., On the deposition of sediment within glacier-influenced fjords: oceanographic controls. Mar. Geol., 1989, 85, 301–329.
[11] Görlich K., Glacimarine sedimentation of muds in Hornsund fjord, Spitsbergen. Ann. Soc. Geol. Pol., 1986, 56, 433–477.
[12] Kowalewski W., Rudowski S., Zalewski S.M., Żakowicz K., Seismostratigraphy of bottom sea sediments in some areas of the Spitsbergen Archipelago. Pol. Polar Res., 1987, 8, 3–23.
[13] Kowalewski W., Rudowski S., Zalewski M., Seismoacoustic studies in Hornsund, Spitsbergen. Pol. Polar Res., 1991, 12, 353–361.
[14] Forwick M., Marine-geological cruise to west Spitsbergen fjords, Cruise Report N-9037. University of Tromsø, Norway, 2007.
[15] Kolondra L., Satellite orthophotomap of a part of South Spitsbergen, Svalbard. University of Silesia, Sosnowiec, 2010.
[16] Moskalik M., Grabowiecki P., Tęgowski J., Żulichowska M., Bathymetry and geographical regionalization of Brepollen (Hornsund, Spitsbergen) based on bathymetric profiles interpolations. Pol. Polar Res., 2013, 34, 1–22.
[17] Moskalik M., Błaszczyk M., Jania J., Statistical analysis of Brepollen bathymetry as a key to determine the average depth on glacier foreland. Geomorphology, 2014, 206, 262–270.
[18] Moskalik M., Tęgowski J., Grabowiecki P., Żulichowska M., Principal Component and Cluster Analysis for determining diversification of bottom morphology based on bathymetric profiles from Brepollen (Hornsund, Spitsbergen). Oceanologia, 2014, 56, 59–84.
[19] Jania J. et al., Lodowce otoczenia Hornsundu [The glaciers of Hornsund region]. In: Kostrzewski A., Pulina M., Zwoliński Z. (Eds.), Glacjologia, geomorfologia i sedymentologia środowiska polarnego Spitsbergenu [Glaciology, geomorphology and sedimentology of Spitsbergen polar environment]. Stowarzyszenie Geomorfologów Polskich, Sosnowiec – Poznań – Longyearbyen, 2004, 68–97. (in Polish)
[20] Birkenmajer K., Spitsbergen, Hornsund Geological Map (1:75 000). University of Silesia, Katowice, 1990.
[21] Karczewski A. et al., Spitsbergen, Hornsund Geomorphology Map (1:75000). University of Silesia, Katowice, 1984.
[22] Blott S.J., Pye K., Gradistat: A grain size distribution and statistics package for the analysis of unconsolidated sediments. Earth Sur. Proc. Land., 2001, 26, 1237–1248.
[23] Folk R.L., The distinction between grain size and mineral composition in sedimentary-rock nomenclature. J. Geol., 1954, 62, 344–359.
[24] Zajączkowski M., Szczuciński W., Plessen B., Jernas P., Benthic foraminifera in Hornsund, Svalbard: Implications for paleoenvironmental reconstructions. Pol. Polar Res., 2010, 31, 349–375.
[25] Zajączkowski M., Sediment supply and fluxes in glacial outwash fjords, Kongsfjorden and Adventfjorden, Svalbard. Pol. Polar Res., 2008, 29, 59–72.
[26] Powell R.D., Molnia B.F., Glacimarine sedimentary processes, facies and morphology of the south-southeast Alaska Shelf and fjords. Mar. Geol., 1989, 85, 359–390.
[27] Dowdeswell J.A., Elverhøi A., Spielhagen R., Glacimerine sedimentary processes an facies on the polar North Atlantic margins. Quaternary Sci. Rev., 1998, 17, 243–272.
[28] Racinowski R., Szczypek T., Wach J., Prezentacja i interpretacja wyników badań uziarnienia osadów czwartorzędowych Presentation and interpretation of the results of grain-size analyses of

quaternary sediments. Wydawnictwo Uniwersytetu Śląskiego, Katowice, 2001. (in Polish)

[29] Powell R.D., Glacimarine processes and inductive lithofacies modelling of ice shelf and tidewater glacier sediments based on Quaternary examples. Mar. Geol., 1984, 57, 1–52.

[30] Powell R.D., Domack E.W., Modern glaciomarine environments. In: Menzies J. (Ed.), Glacial Environments, Vol. 1: Modern Glacial Environments: Processes, Dynamics and Sediments. Butterworth-Heinemann, Oxford, 1995, 445–486.

[31] Elverhøi A., Roaldset E., Glaciomarine sediments and suspended particle matter, Weddell Sea Shelf, Antarctica. Polar Res., 1983, 1, 1–21.

[32] Syvitski J.P.M., Andrews J.T., Dowdeswell J.A., Sediment deposition in an iceberg-dominated glacimarine environment, East Greenland: basin fill implications. Global Planet. Change, 1996, 12, 251–270.

[33] Elverhøi A., Lønne O., Seland R., Glaciomarine sedimentation in a modern fjord environment, Spitsbergen. Polar Res., 1983, 1, 127–149.

[34] Elverhøi A., Glacigenic and associated marine sediments in the Weddell Sea, fjords of Spitsbergen and the Barents Sea: a review. Mar. Geol., 1984, 57, 53–88

[35] Plassen L., Tore O., Forwick M., Integrated acoustic and coring investigation of glacigenic deposits in Spitsbergen fjords. Polar Res., 2004, 23, 89–110.

[36] Moskalik M., Forwick M., Vorren T.O., Bathymetry and slope gradients of Brepollen (Hornsund, Spitsbergen). Paper presented at the ART-APECS Sciences Workshop Overcoming challenges of observation to model integration in marine ecosystem response to sea ice transitions, Sopot, Poland, 23-26 October, 2012.

[37] Kehrl L.M., Hawley R.L., Powell R.D., Brigham-Grette J., Glacimarine sedimentation processes at Kronebreen and Kongsvegen, Svalbard. J. Glaciol., 2011, 57, 841–847.

[38] Cofaigh C.O., Dowdeswell J.A., Laminated sediments in glacimarine environments: diagnostic criteria for their interpretation. Quaternary Sci. Rev., 2001, 20, 1411–1436

[39] Węsławski J.M., Zajączkowski M., Moroz R., Kwa'sniewski S., Preliminary report from the cruise of m/s 'Jantar' to South Spitsbergen area – August 1984. Polish Academy of Sciences, Sopot, 1985.

[40] Baranov S., Modeling and simulating an aftershock process caused by a strong earthquake in the Barents Sea shelf. Russ. J. Earth Sci., 2011, 12, ES1002.

[41] Moskalik M., Pastusiak T., Tęgowski J., Multibeam Bathymetry and Slope Stability of Isvika Bay, Murchisonfjorden, Nordauslandet. Mar. Geod., 2012, 35, 389–398.

[42] Lønne I., Sedimentary facies and depositional architecture of ice-contact glaciomarine systems. Sediment. Geol., 1995, 98, 13–43.

[43] Ottesen D., Dowdeswell J.A., Assemblages of submarine landforms produced by tidewater glaciers in Svalbard. J. Geophys. Res., 2006, 111, F01016.